Robust Control Design for a Parallel Resonant Converter using μ-Synthesis

Juanyu Bu[†]   Mario Sznaier[†1]   Issa Bartarseh[‡]   Zi-Qin Wang[†]

[†] Department of Electrical Engineering
Pennsylvania State University
State College, PA 16802

[‡] Department of Electrical and Computer Engineering
University of Central Florida
Orlando, FL 32816

Abstract

Because of their reduced switching loss, dc-to-dc resonant converters have been widely used in the design of small size and light weight power supplies. The steady state and dynamic behaviors of the conventional series and parallel resonant converters have been thoroughly analyzed, as well as the small signal models around given nominal operating points have been obtained. These models have been used in the past to design controllers to keep the output voltage constant in presence of input perturbations. However, these controllers did not take into account components and load variations, which could lead to instability problems. Furthermore, the prediction of frequency range for stability was done in a posteriori, either experimentally or by a trial-and-error approach. In this paper, we use μ-synthesis to design a robust controller for the second-order conventional parallel resonant converter. In addition to robust stability under different load conditions, the design objectives also include rejectionr of disturbances at the converter input while keeping the control input and settling time within values compatible with practical implementation.

1 Introduction

Due to their reduced switching losses, the dc-to-dc resonant converters are currently the object with widespread interests among power conversion applications. In resonant converters, high operating frequencies are used since they result in smaller, lighter magnetic components, lower harmonic contents and faster transient response. Because of all these features, the high frequency resonant converters are becoming the preferred choice in applications requiring high-efficiency, high-density, dc-to-dc power converters[21].

In the past controllers for resonant converters were designed to keep the output voltage constant in the presence of input perturbations. However, neither load nor components variations were considered in these controllers. In this work we use μ-synthesis[1] to design a robust controller for a second-order parallel resonant converter (PRC). The design objective is to robustly reject input variations in the presence of load and components uncertainties, while keeping small control actions and short settling time. This is accomplished by selecting appropriate weight functions reflecting these requirements.

*Author to whom correspondence should be addressed. Phone: 814-865-2364. Fax: 814-865-7065. E-mail: msznaier@frodo.ee.psu.edu

2 Problem Description

2.1 The Second-order Parallel Resonant Converter[2]

The half-bridge Capacitively Coupled second-order PRC is illustrated in Figure 1. Two capacitors C_i are assumed much larger than the resonant capacitor $C(C_i \gg C)$. Hence they act like a voltage divider, with their voltages V_g's equal to one-half of the source voltage E. The combinations of the diodes and transistors form the bi-directional switches, which operate at 50% duty ratio to generate a symmetrical square wave voltage V_s with switching frequency f_s, applied across the resonant tank LC. The full wave rectifier is used in the output circuit to couple the resonant capacitor voltage v_c to the load R_o. A very large output inductor L_o is needed to minimized the load effect on the resonant capacitor voltage and to ensure the constant amplitude of the current through the output circuit. The following nominal parameters are taken from the design example in Chapter 2 of [2]:

$$
\begin{aligned}
L &= 41.18\mu H \\
C &= 11.30nF \\
L_o &= 10mH \\
R_o &= 208.33\Omega \\
V_g &= 100V \\
V_o &= 250V \\
f_s &= 200kHz \\
Z_o &= \sqrt{L/C} = 60.39\Omega
\end{aligned}
$$

For convenience, we introduce the following normalized variables:

$$
\begin{aligned}
V_{ng} &= \frac{V_g}{V_g} = 1; \\
Q_p &= \frac{R_o}{Z_o} = 3.45; \\
V_{no} &= \frac{V_o}{V_g} = 2.5; \\
F_{ns} &= \frac{f_s}{f_o} = 0.86.
\end{aligned}
$$

where the resonant frequency $f_o = \frac{1}{2\pi\sqrt{LC}}$

2.2 Small Signal Model

The converter is a nonlinear, variable structured system. For a given operating point, a discrete-time small signal model can be

289
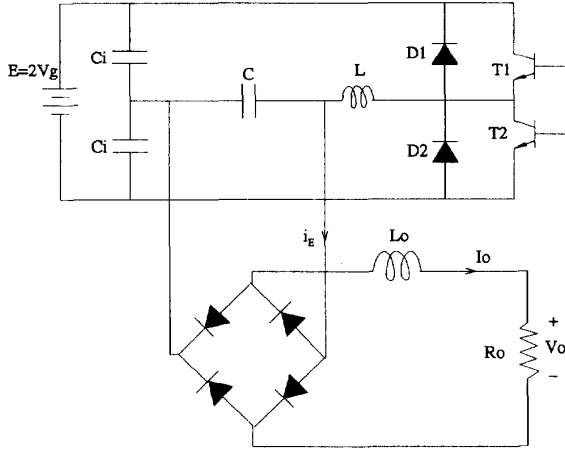
Figure 1: The 2nd-order PRC circuit diagram

obtained by using perturbation methods[17]. The sampling time for this discrete-time model is equal to $T_s/2$, where $T_s = 1/f_s$ is the switching period. Therefore, from sampling theory it follows that this model is correct under small signal perturbations with frequencies up to the operating switching frequency f_s.

The discrete model from F_{ns} and V_{ng} to output V_{no} at the nominal operating point is given by the following state space realization:

$$X(k+1) = AX(k) + BU(k)$$
$$Y(k) = CX(k)$$

where

$$A = \begin{pmatrix} 0.8219 & 0.5504 & -2.1402 \\ -0.2767 & 0.6108 & -0.6644 \\ 0.0053 & 0.0075 & 0.9387 \end{pmatrix},$$

$$B = \begin{pmatrix} -6.4684 & 0.4834 \\ 10.6774 & 1.9499 \\ -0.0002 & 0.0162 \end{pmatrix},$$

$$C = \begin{pmatrix} 0 & 0 & 3.45 \end{pmatrix}$$

The state variables and input are defined as

$$X(k) = \begin{bmatrix} i_{nl}(k) & v_{nc}(k) & I_{no}(k) \end{bmatrix}^T,$$

$$U(k) = \begin{bmatrix} F_{ns}(k) & V_{ng}(k) \end{bmatrix}^T$$

where i_{nl}, v_{nc} and I_{no} are the normalized resonant inductor current; capacitor voltage and output current, respectively.

2.3 Control Objectives

The purpose of the feedback control is to keep the output voltage at a prescribed level (in our case $V_o = 250V$, i.e. $V_{no} = 2.5$) at all operating points, using as control input the switching frequency f_s. This problem can be further divided into three parts:

a. Line Regulation: The line voltage variation, modeled as an external disturbance, leads to a disturbance rejection problem.

b. Load Regulation: Load variations will appear as model uncertainty and could possibly lead to stability problems.

c. The requirement of satisfactory transient responses under line voltage variation and/or load change within the whole operating range.

In addition, all physical variables should be limited to practical values in order to ensure the implementability of the resulting controller. Since all these control objectives must be achieved for possible values of components and load conditions, this constitutes in fact a robust performance problem.

3 Analysis of the Plant

3.1 Control Characteristics

The effects of switching frequency changes and load variations upon the converter output can be seen from the relationships among V_{no}, F_{ns} and Q_p, which are known as control characteristics[2]. Figure 2 illustrates the control characteristics curves for different load Q_p's, where the mark '*' indicates the nominal operation point. As shown in the figure, at heavier load(large Q_p), the output voltage will change faster with respect to the frequency variation. This results in tougher control problem at heavy load conditions. Our control objective is to keep the converter operating along the dashed line in Figure 2 with constant output V_{no} in the presence of input perturbations and load variations.
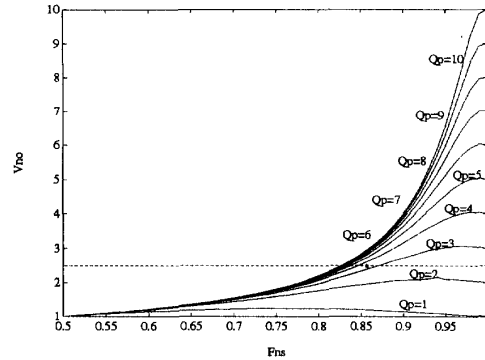
Figure 2: The Conventional PRC Control Characteristics Curves

3.2 Frequency Responses

From the discrete time state-space model, we can easily get the z-transfer functions from the normalized switching frequency F_{ns} and the normalized line input V_{ng} to the normalized output V_{no}:

$$\begin{pmatrix} G(z) & G_g(z) \end{pmatrix} = \begin{pmatrix} \frac{V_{no}(z)}{F_{ns}(z)} & \frac{V_{no}(z)}{V_{ng}(z)} \end{pmatrix}$$
$$= C[zI - A]^{-1}B \qquad (1)$$

290

Finally, a transfer function in the frequency domain s can be obtained by using a bilinear transformation with the sample time $T_s/2$:

$$z = \frac{1 + sT_s/4}{1 - sT_s/4} \quad (2)$$

We denote the nominal transfer functions in s as $G(s)$ and $G_g(s)$. They are given by:

$$
\begin{aligned}
G(s) &= 2.652 * 10^{-2} \frac{s + 795041}{s + 29167} \\
&\quad * \frac{(s - 792431)(s - 800003)}{(s + 83363 \pm 202487i)} \quad (3) \\
G_g(s) &= -1.367 * 10^{-2} \frac{s - 800003}{s + 29167} \\
&\quad * \frac{(s + 484930 \pm 290253i)}{(s + 83363 \pm 202487i)} \quad (4)
\end{aligned}
$$

The frequency responses of $G(s)$ at the nominal operating point as well as at a few other load conditions are shown in Figure 3. As shown in the figure, when the load becomes heavier(larger R_o), the overshoot increases, resulting in a more difficult control problem. On the other hand, the control characteristics require that Q_p be greater than V_{no} in order to get the prescribed output voltage. That means that R_o should be greater than 151Ω. Therefore, in this paper we assume that R_o will vary within the range of 151Ω to 1200Ω.
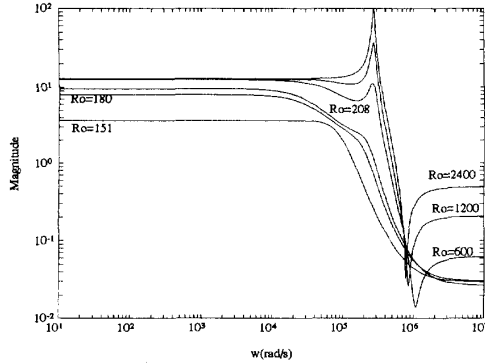
Figure 3: Frequency responses G(s) at different load conditions

4 Control Design

4.1 Structured singular value and μ-synthesis

Consider the standard 'M-Δ' structure shown in Figure 4, where M is a compatible matrix and $\Delta = diag\{\Delta_p\}$ represents a model perturbation with a block diagonal structure. The structured singular value μ is defined as [1]:

$$\mu_\Delta^{-1}(M) = \min_\Delta\{\bar{\sigma}(\Delta)|det(I + M\Delta) = 0\} \quad (5)$$

As shown in [1], if M is a stable transfer matrix, a necessary and sufficient condition for robust stability of the interconnected
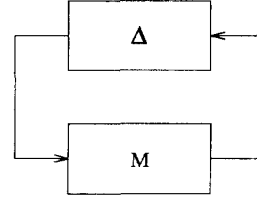
Figure 4: Standard "M-Δ" structure

systems for all perturbations $\|\Delta\|_\infty \leq 1$ is that $\mu(M) < 1$. Robust performance can be addressed by introducing an additional fictitious perturbation block. It can be shown [1] that robust performance is achieved if and only if:

$$\mu_{RP} = \sup_\omega \mu_\Delta(M) < 1 \quad (6)$$

where Δ contains both the uncertainty and the performance blocks. The problem of finding a stabilizing controller which minimizes μ_{RP}, (μ-synthesis), is not fully solved yet. The present μ synthesis algorithm, called D-K iteration, is a combination of H_∞ synthesis and the optimal D-scaling. Although global convergence is not theoretically guaranteed, the algorithm works well in practice.

4.2 Weights Selection[12][13]

To cover all possible plants, the uncertainty descriptions and weights must be specified. The load variation is a primary source for uncertainties. Let $G^{R_o}(s)$ denote the transfer function from control input F_{ns} to output V_{no} at operating points $R_o \neq 208.33\Omega$. Then the multiplicative uncertainty can be expressed as

$$l^{R_o}(W) = |(G^{R_o} - G)G^{-1}| \quad (7)$$

Some sample uncertainties for different load R_o are shown in Figure 5. In order to keep the complexity of the controller reasonably low, we will cover all multiplicative uncertainties due to load changes from 151Ω to 1200Ω with the following first order weight:

$$W_I(s) = \frac{1.3 * 10^{-4}s + 0.62}{10^{-6}s + 1} \quad (8)$$

The frequency response of $W_I(s)$ is also shown in Figure 5. Additionally, there may be some component uncertainties. However, they result in changes on Q_p which can be effectively considered as load R_o changes.

To achieve the control objectives, we also need to choose the performance weights $W_e(s)$ and $W_u(s)$, which are associated with the tracking/regulation error and the control effort respectively. The selection of $W_e(s)$ and $W_u(s)$ entails a trade-off among different performance requirements, particularly good regulation versus peak control action. The following weights are used in design:

$$W_e(s) = \frac{1}{4}\frac{0.001s + 1}{0.001s} \quad (9)$$

$$W_u(s) = \frac{1 * 10^{-4}s}{2 * 10^{-7}s + 1} \quad (10)$$

The weight on the error $W_e(s)$ was selected to be an integrator at low frequencies in order to get zero steady-state error
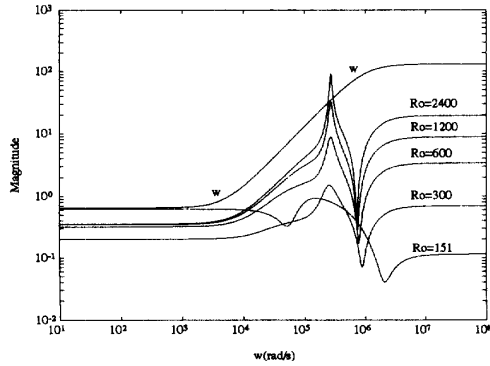
Figure 5: Multiplicative uncertainty for different load R_0 and uncertainty weight

and good tracking. It gives a close-loop bandwidth of approximately $1000rad/s$. However, it also allows an amplification of 4 for high frequency noise. The weight on the control input $W_u(s)$ was chosen close to a differentiator to penalize fast changes and large overshoot in the control input.

4.3 μ-optimal controller
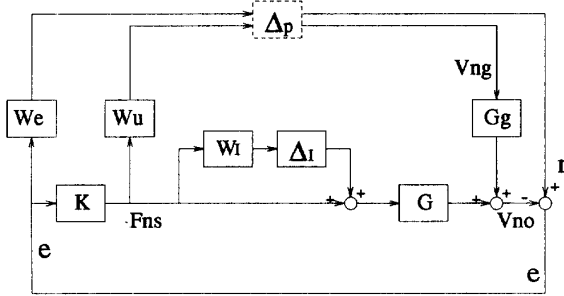
Figure 6: The block diagram for μ-synthesis

By using the uncertainty description and performance weights developed in section 4.2, we get an uncertainty structure Δ with a scalar block (corresponding to the uncertainty) and a 2x2 block (corresponding to the performance). The block diagram for μ synthesis is shown in Figure 6. By using μ-toolbox[1], we obtained a 10th-order μ-optimal controller with $\mu_{RP} = 0.9843 < 1$, thus guaranteeing robust performance. Model reduction yielded a 5th order controller with no performance degradation($\mu_{RP} = 0.9846 < 1$). The state space realization of the reduced order controller is:

$$K = C_k(sI - A)^{-1}B_k + D_k \qquad (11)$$

where
$A_k =$

$$\begin{pmatrix} -0.25 & 2.487 & -1.235 & -0.0419 & 1.543 \\ 2.487 & -283526 & 416158 & 7336 & 384402 \\ 1.235 & -416158 & -216013 & -210276 & 427561 \\ -0.0419 & 7336 & 210276 & -266.8 & 27402 \\ 1.543 & -384402 & -427561 & 27402 & 1284619 \end{pmatrix}$$

$$B_k^T = (\ -14.23 \quad 70.78 \quad 35.14 \quad -1.191 \quad 43.91\ )$$

$$C = (\ -14.23 \quad 70.78 \quad -35.14 \quad -1.191 \quad 43.91\ )$$

$$D_k = 6.578e - 9$$

The s-domain transfer function of the resulted controller is obtained as:

$$K(s) = \frac{K_{num}(s)}{K_{den}(s)} \qquad (12)$$

where

$$
\begin{aligned}
K_{den}(s) &= s^5 + (1.784e+6)s^4 + (8.865e+11)s^3 \\
&\quad + (2.204e+17)s^2 + (2.727e+22)s + (6.817e+21) \\
K_{num}(s) &= (6.578e-9)s^5 + (2.051e+3)s^4 + (1.075e+10)s^3 \\
&\quad + (1.814e+15)s^2 + (4.747e+20)s + (5.522e+24)
\end{aligned}
$$

5 Simulation Results

The linearized model described in section 2 is correct only with small signal perturbations. Therefore, the close-loop system was simulated under 20% step change in line voltage V_{ng} and reference input r. Figures 7 and 8 show the transient responses of the system due to these changes. To verify the robust performance, the linear simulations were done at nominal operating point $Ro = 208\Omega$ and two extreme cases $R_o = 151\Omega$ and 1200Ω.
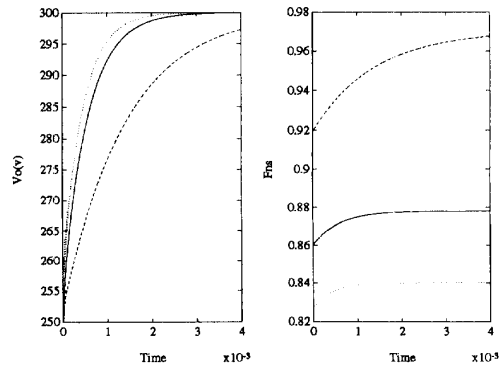
Figure 7: Linear Simulation Results for Reference Step Change(20%): $R_o = 208\Omega(solid), 151\Omega(dash)$ and $1200\Omega(dot)$

As shown in the simulation results, the settling time at nominal case is about 3msec., while for $R_o = 151\Omega$ and 1200Ω the settling time is 4msec. and 2.5msec. respectively. The output response satisfies the design objectives. However, we also notice that at the heaviest load($R_o = 1200\Omega$), there are some high frequency oscillations in both the output and control input

corresponding to reference and line step change. These oscillations(or chattering) are due to the neglected high frequency uncertainties and limitation of the small signal modelling approach. They can be attenuated by increasing the weight on the high frequency range, but this will prevent finding a controller guaranteeing robust performance for all possible load conditions. That is always the dilemma for robust control: the tradeoff between robustness and performance.
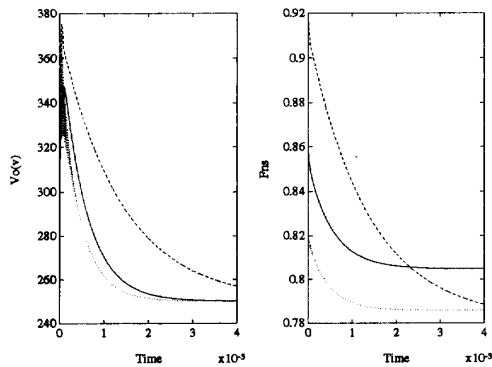
Figure 8: Linear Simulation Results for Line Voltage Step Change(20%): $R_o = 208\Omega(solid), 151\Omega(dash)$ and $1200\Omega(dot)$

6 Conclusions

The paper shows that the μ-robust control provides a very powerful tool for synthesizing controllers for resonant converters, capable of guaranteeing good performance under a wide range of load conditions.

References

[1] G. J. Balas et al. μ-Analysis and Synthesis Toolbox, April 1991.

[2] Issa Batarseh. *Analysis and Design of High Order Resonant Converters*. PhD Dissertation, University of Illinois-Chicago, June 1990.

[3] Issa Batarseh and C. Q. Lee. Steady-State Analysis of the Parallel Resonant Converter with LLCC-type Commutation Network. In *IEEE Transactions on Power Electronics*, 6(3), 525-538, July 1991.

[4] Issa Batarseh and R. Severns. Resonant Converter Topologies with Three and Four Energy Storage Elements. submitted to *IEEE Transactions on Power Electronics*.

[5] A. S. Bhat and S. B. Dewan. A Generalized Approach for the Steady State Analysis of Resonant Converters. In *Proceedings of IEEE-APEC'86*, 664-771, 1986.

[6] John C. Doyle. Analysis of Feedback Systems and Structured Uncertainties. In *IEE Proceedings, Part D*, 129(6), 242-250, 1982.

[7] S. Freeland. *An Introduction to the Principle and Features of Resonant Power Conversion*. Rockwell International Corporation–Autometics ICBM Systems Division, Anaheim, CA, 1988.

[8] S. Johnson and Erickson. Steady-State Analysis and Design of the Parallel Resonant Converters. In *IEEE PESC'86*, 154-165, 1986.

[9] J. Kassakian and M. Schlecht. High Frequency High Density Converters for Distributed Power Supply Systems. In *Proceedings of IEEE*, 76, 4, April 1988.

[10] C. Q. Lee and Issa Batarseh. Performance Characteristics of Parallel Resonant Converter. In *IEEE PESC'86*, 154-165, 1986.

[11] K. Liu, R. Oruganti and F. C. Lee. Quasi-Resonant Converters: Topologies and Characteristics. In *IEEE Transactions on Power Electronics*, 2(1), 62-71, 1987.

[12] P. Lundstrom, S. Skogestad and Zi-Qin Wang. Performance Weight Selection for H_∞ and μ-Control Method. In *Transactions of the Institute of Measurement and Control*, 13(5), 241-252, 1991.

[13] P. Lundstrom, S. Skogestad, and Zi-Qin Wang. Uncertainty Weight Selection for H_∞ and μ-Control Methods. In *Proceedings of IEEE Conference on Decision and Control*, Brighton, December 1991.

[14] R. Oruganti. *State-Plane Analysis of Resonant Converters*. PhD Dissertation, Virginia Polytechnic Institute and State University, August 1987.

[15] R. Oruganti and F. C. Lee. State-Plane Analysis of Parallel Resonant Converter. In *IEEE PESC'85*, 56-73, 1985.

[16] Andy Packard, John C. Doyle and Gary Balas. Linear, Multivariable Robust Control with a μ Perspective. In *Transactions of the ASME*, volume 115, June 1992.

[17] K. Siri. *Analysis of Resonant Converters and Control Approaches for Parallel Connected Converter Systems*. PhD Dissertation, University of Illinois-Chicago, July 1991.

[18] R. L. Steigerwald. A Comparison of Half-Bridge Resonant Converter Topologies. In *IEEE Transactions on Power Electronics*, 3(2), 174-182, 1988.

[19] V. Vorperian. *Analysis of Resonant Converters*. PhD Dissertation, California Institute of Technology, May 1984.

[20] Zi-Qin Wang, Mario Sznaier, Issa Batarseh, and Juanyu Bu. Robust Control Design for a Conventional Series Resonant Converter Using μ-Synthesis. In *2nd IEEE Conference on Control Applications*, 1993.